Quaternary Science Reviews 220 (2019) 142–153

Contents lists available at ScienceDirect

Quaternary Science Reviews

journal homepage: www.elsevier.com/locate/quascirev

Paleoclimatology of the Levant from Zalmon Cave speleothems, the northern Jordan Valley, Israel

Jonathan Keinan [a, b, *], Miryam Bar-Matthews [a], Avner Ayalon [a], Tami Zilberman [a], Amotz Agnon [b], Amos Frumkin [b, c]

[a] Geological Survey of Israel, Yisha'ayahu Leibowitz St. 32, Jerusalem, Israel
[b] Institute of Earth Sciences, The Hebrew University, Jerusalem 91904, Israel
[c] Cave Research Center, The Hebrew University, Jerusalem 90627, Israel

ARTICLE INFO

Article history:
Received 2 October 2018
Received in revised form
10 July 2019
Accepted 10 July 2019

Keywords:
Quaternary
Paleoclimate
Dead Sea Rift Valley
Speleothems
Stable isotopes
U-Th series

ABSTRACT

The Levant region of Israel, located along the Eastern Mediterranean Sea, is characterized by Mediterranean climate, but sixty km eastwards towards the Dead Sea Rift Valley (DSRV), the region rapidly becomes a 'rain shadow' desert. Speleothems from the Mediterranean climate zone continuously grew throughout several glacial/interglacial cycles, indicating that water was always available in the unsaturated zone. Their $\delta^{18}O$ variations match global and regional climate changes, with the Eastern Mediterranean Sea being the major control on their $\delta^{18}O$ values, as evident from the similarity between the speleothems and the planktonic foraminifer *G. ruber* records. In contrast, speleothems along the central and southern segments of the DSRV grew mainly during last glacial periods coinciding with the higher stands of Lake Lisan, the precursor of the present-day Dead Sea. This paper discusses the newly discovered Zalmon Cave speleothems, located in the northern segment of the DSRV shedding light on the hydrological conditions along the rift during last glacial. Unlike speleothems located further south along the DSRV, Zalmon Cave speleothems grew both during glacial and interglacial periods. However, during last glacial their $\delta^{18}O$ values, shifted to lower values by ~1–2‰ relative to speleothems from central Israel coinciding also with the largest difference in $\delta^{18}O$ values between Zalmon Cave speleothems and the marine record. The data suggest that a change of the westerlies' storm tracks occurred during most of the last glacial period, which resulted in increased rainfall in the northern DSRV providing freshwater input during the otherwise relatively 'drier' glacial.

1. Introduction

1.1. Speleothems in the Eastern Mediterranean (Levant) region as paleoclimate records

Calcite speleothems are unique archives for paleoclimate reconstruction. They provide both the required accurate and precise U-Th series chronology together with proxy data (e.g. growth intervals and rate, isotopic composition and timing of isotopic changes), which serve as paleoclimate indicators (e.g. Bar-Matthews et al., 1997, 2000, 2003; Cheng et al., 2000; Shen et al., 2002; Vaks et al., 2006, 2007). The isotopic and geochemical compositions of speleothems can testify for ocean-atmosphere-land connections, changes in local rainwater source, local temperatures, precipitation amounts, groundwater characteristics, and soil-water-rock interactions (e.g. Bar-Matthews et al., 2000, 2003; Ayalon et al., 2002, 2013; McGarry et al., 2004; Kolodny et al., 2005; Affek et al., 2008; Verheyden et al., 2008).

A detailed record of climatic changes in the Levant - Eastern Mediterranean region for the last 225 ka was established through speleothems studies combining U-Th dating with stable isotopic compositions, and this record has been compared with the Eastern Mediterranean marine record, pollen and lake sediments as reviewed by Bar-Matthews (2014) and Bar-Matthews et al. (2017) (Fig. 1). These speleothem studies cover different climatic zones, and their findings clearly demonstrate that speleothem isotopic compositions capture global climatic diversity, changes, and teleconnection processes. Comparisons and correlations between different areas are crucial to understanding the spatial and

* Corresponding author. Geological Survey of Israel, Yisha'ayahu Leibowitz St. 32, Jerusalem, Israel.
E-mail address: jonathan.keinan@mail.huji.ac.il (J. Keinan).

https://doi.org/10.1016/j.quascirev.2019.07.018
0277-3791/

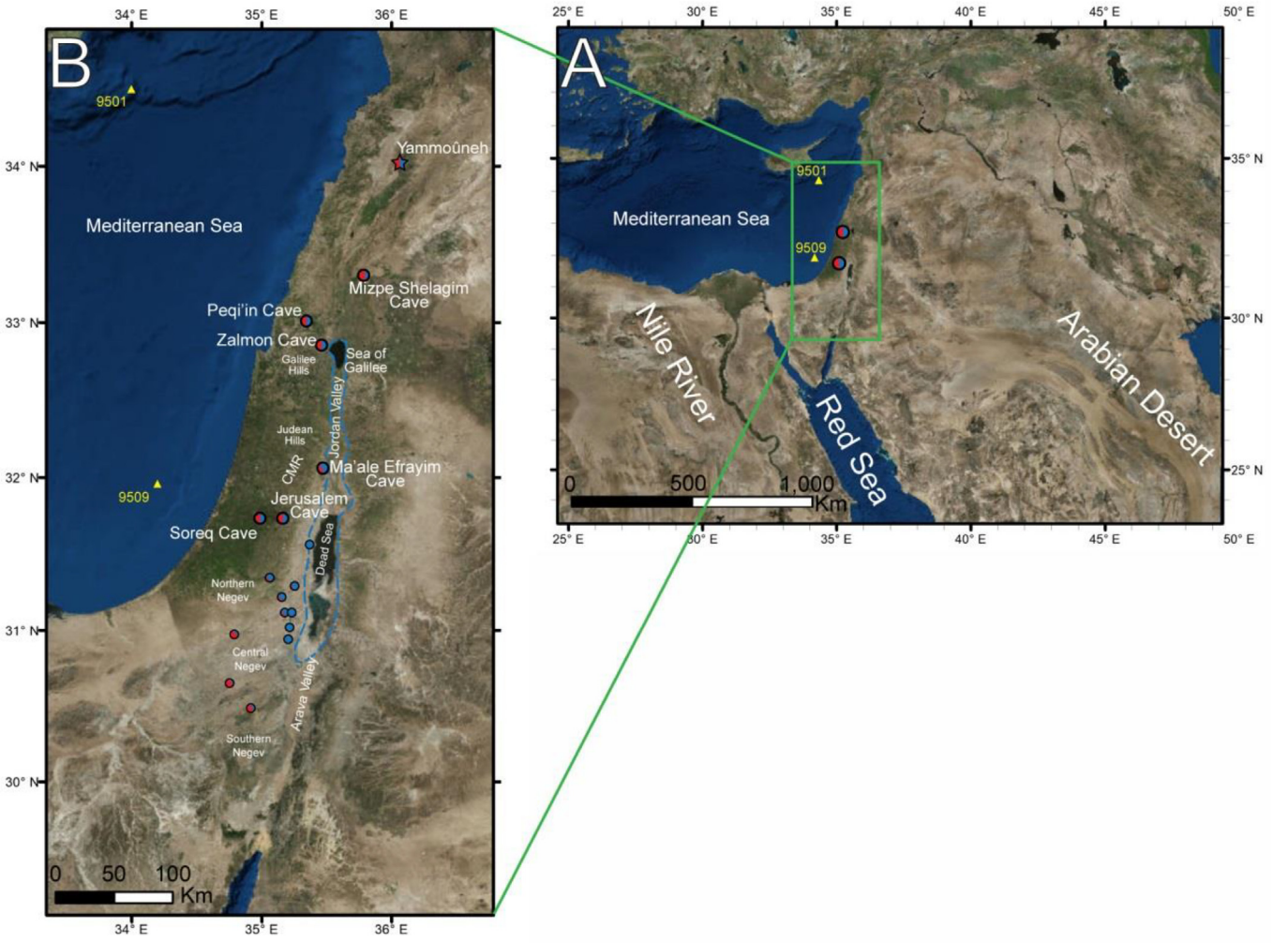

Fig. 1. Regional map and locations of the study sites described in the text (B is an enlargement of the green rectangle in A). Study sites are color coded: blue – "wet" during glacial periods, red – "wet" during interglacial periods. Circles mark caves. Blue and red circles mark caves with continuous speleothems deposition. Lakes are marked by a star and marine drilled core sites by yellow triangles. The blue line marks the area of Lake Lisan during its highest stand (modified after Torfstein et al., 2013). (For interpretation of the references to colour in this figure legend, the reader is referred to the Web version of this article.)

chronological changes of climate. Differences in the isotopic composition of speleothems deposited during the same time interval and periods of growth vs. non-growth of speleothems from various parts of the Levant clearly demonstrate that regional differences are climatically driven (e.g., Bar-Matthews et al., 2017).

The various studies of Levant speleothems have shown that it is possible to reconstruct a rainfall precipitation map covering both glacial and interglacial periods in a region with steep north-south and west-east precipitation gradients, ranging from more than 800 mm yr^{-1} to less than 50 mm yr^{-1} over a distance of 300 km. In central and northern Israel (the Judean Hills and Galilee) speleothem deposition was continuous during both glacials and interglacials and points to continuous water availability. However, speleothems within the Dead Sea Rift Valley (DSRV), in the rain shadow semi-arid Southern Jordan Valley, mostly deposited during glacial periods (Lisker et al., 2010). Their growth clearly indicates that a positive water balance during glacials allowed more water to enter the unsaturated zone. In the central Jordan Valley at Ma'ale Efrayim Cave (ME), deposition during glacials was intensive with moderate deposition also occurring during peak interglacials (Vaks et al., 2003), suggesting wetter glacials along the central DSRV compared to modern day arid climate.

Such observations coupled with regional temperature variations over glacial-interglacial cycles led to the proposition that the minimum amount of annual precipitation required for speleothem deposition is 300–350 mm during interglacial periods and 200–275 mm during glacial periods (Vaks et al., 2006, 2010). The glacial period isotopic profiles of Soreq Cave and ME Cave located on opposite flanks of the central mountain ridge show a high correlation, implying a similar source of rain for both regions during this time. This conclusion is supported by similar $\delta^{13}C$ values in both caves, indicating similar vegetation types. The similar isotopic profiles indicate that during the lower temperature glacial periods, the amount of rainfall in the DSRV was either larger and/or similar to the western side of the central mountain ridge (Vaks et al., 2003; Goldsmith et al., 2016). The transition from the colder glacial conditions to the warmer interglacial periods in the ME region was characterized by temperature increase and rising aridity in the Jordan Valley.

In contrast, speleothem growth in Central and Southern Negev

Desert (the north-eastern corner of the Sahara Desert, Fig. 1) ceased during glacials and mostly occurred during peak interglacials. These periods, defined as Negev Humid Periods (NHP) (Vaks et al., 2006, 2007, 2010), are characterized by extensive deposition of speleothems with low $\delta^{18}O$ values. The frequency of depositional episodes and thickness of individual laminae decreases southwards, implying a general decrease in rainfall from north to south (Vaks et al., 2010), similar to the present-day precipitation trend. Speleothem deposition in the northern Negev Desert occurred during both glacial and interglacial periods (Vaks et al., 2010) suggesting that the desert boundary migrated ~30–50 km southward and eastward during glacial intervals relative to its present-day position (Bar-Matthews, 2014).

In the extreme north, Mount Hermon, the southernmost point of the Alpine-type karst extending from Turkey to Syria and Lebanon, receives most of its precipitation as snowfall. Speleothem deposition in Mizpe Shelagim Cave (Fig. 1) located on Mount Hermon at 2200 m altitude was continuous during interglacials and restricted to short warming episodes during the last glacial period (Ayalon et al., 2013). Based on fluid inclusion studies, speleothem growth was restricted to periods with temperatures above 3 °C (Ayalon et al., 2013).

1.2. Quaternary paleo-lakes and their climatic implications

The overall picture that emerges from lakes in the Middle East and North Africa shows that the wettest phases occurring during peak interglacials, coincide with sapropel deposition in the Eastern Mediterranean Sea and wet intervals in Lebanon, northeastern Turkey (Lake Van), northeast Sahara and Arabia, as evident from speleothem and lacustrine records (Rossignol-Strick, 1985; Fleitmann et al., 2003a,b, 2011; Develle et al., 2010, 2011; Litt et al., 2014; Stockhecke et al., 2014; Gasse et al., 2015; Nehme et al., 2015). A different scenario emerges from the precursor sediments of the Dead Sea, located on the lower eastern flanks of the central mountain ridge (Bartov et al., 2002; Torfstein et al., 2009; Waldmann et al., 2009), which showed their highest stands during glacials rather than peak interglacials. Kolodny et al. (2005) and Enzel et al. (2008) argue that the lake-level changes are a gauge for wetter/drier climate, and that the existence of the larger Lake Lisan (precursor of the Dead Sea) during glacials requires significantly more rainfall, making the glacial climate in the Dead Sea region moister than the interglacial climate. Enzel et al. (2008) suggest that unlike today, Eastern Mediterranean cyclones during the glacial were forced south by the ice and snow-covered Europe and Turkey, causing rain to be funneled directly eastward along the Mediterranean Sea into the Levant, leading to more precipitation.

This latter view, however, does not explain why other lake records, especially the Yammoûneh sequence in the northern Levant (Fig. 1), show a different picture of dry glacial conditions (Develle et al., 2010, 2011). It remains an open question whether the hydrological differences between the lake records are a result of local factors or due to a change in the north–south rainfall gradient and the southward migration of the westerly belt (Develle et al., 2011).

The aim of this study is to use speleothem deposition periods alongside their stable isotopic composition from the newly discovered Zalmon Cave in the eastern Galilee region, to unravel the paleoclimate conditions along the DSRV, and to understand the spatial paleoclimate variations in the Levant. Zalmon Cave is distinctively located on the boundary between the Galilee Mediterranean climatic regime and that of the northern segment of the DSRV (Fig. 1), thus allowing us to fill an important gap in the records of the south and the north DSRV.

2. Zalmon Cave: geological setting

Zalmon Cave, discovered in October 2013, is located in the northern part of the Dead Sea catchment. It is approximately 8 km west of the Sea of Galilee (Fig. 1) within the karstic Turonian B'ina Formation (Arkin et al., 1965; Bogoch and Sneh, 2008). The entrance to the cave is 23 m above sea level and approximately 35 km east of the Mediterranean Sea. The climate in the region is Mediterranean, with average annual precipitation of ~550 mm and an annual temperature average of 21 °C (IMS - Israel Meteorological Service, 2011). The cave is an isolated chamber, a type of cavity common in Israel (Frumkin and Fischhendler, 2005) that had been disconnected from the surface until its exposure as a result of the road construction. It is intensively decorated with speleothems, which often conceal the original morphology, containing several types of calcite dripstones, such as stalactites and stalagmites, as well as a variety of cave corals. Much of the cave exhibits evidence of disturbance, possibly due to seismic activity in the form of broken and re-welded stalagmites, stalagmites which have a change of growth axis due to tilting, stalactites and collapsed ceiling embedded in flowstones, and cracks refilled with calcite precipitation (Kagan et al., 2005). The cave was mapped shortly after its discovery by the Cave Research Center (Fig. S1 in the Supplementary material for cave map and cross sections).

The significance of this cave location is threefold:

- Situated on the border between the DSRV and the Galilee, Zalmon Cave speleothems constrain the paleoclimate gradients further north from the Dead Sea along the DSRV.
- Situated on the cross-roads between Mediterranean climate and the 'rain shadow' region, information from Zalmon Cave speleothems enables us to correlate between Mediterranean westerlies and paleoclimate along the northern part of the Dead Sea region.
- Zalmon Cave is located off the northern catchment of Lake Lisan and its precursor lakes, offering a potential insight into the hydrological conditions during its high glacial stands.

3. Methodology

3.1. Speleothem sampling

In order to gain data on growth periods and high resolution paleoclimate changes, we collected eight relatively well preserved stalagmites from within the cave. They were mapped, photographed and removed with as minimal damage as possible. The speleothems were sectioned at the Geological Survey of Israel (GSI) using a diamond saw and polished in order to expose their internal structure. Speleothems with laminar texture and minimal evidence for secondary alteration (Bar-Matthews et al., 1997) were dated and studied for their oxygen and carbon isotopic composition and petrography.

3.2. Petrography

Speleothems were cut and polished to make thin sections. The petrography and mineralogy were studied using an Olympus BX50 polarizing microscope at the GSI, in order to check for impurities, locate hiatuses and identify crystal habitat (Frisia, 2015) (Fig. S2).

3.3. U-Th dating

For dating purposes, a diamond drill was used in order to excavate 0.2–0.3 g of sampling material along the growth axis

(Fig. S2). U-Th dating was done at the GSI using a Nu Instruments Ltd (UK) Multi-Collector-Inductively-Coupled-Plasma-Mass-Spectrometer (MC-ICP-MS) equipped with 12 F cups and 3 ion counters. The procedures for extraction and purification of U and Th as well as methodology of U-Th dating using MC-ICP-MS are described in detail by Vaks et al. (2006), Bar-Matthews and Ayalon (2011), Grant et al. (2012) and Hershkovitz et al. (2015).

3.3.1. Age corrections

Kaufman et al. (1998) argued that ages obtained from samples with $^{230}Th/^{232}Th < 30$ require correction. Above this ratio the correction becomes negligible compared to the analytical uncertainty of the measurement. Li et al. (1989) and Richards and Dorale (2003) argued for thresholds of between 100 and 300 in the case of Thermal Ionization mass spectrometer dating. Fortunately, many of the samples from Zalmon Cave have $a^{230}Th/^{232}Th > 100$ so a correction was not necessary. A total of 102 samples were dated. Seven have $a^{230}Th/^{232}Th$ ratio of less than 30 and another 23 have $a^{230}Th/^{232}Th$ ratio between 30 and 100. For samples with $a^{230}Th/^{232}Th < 100$ a correction factor of 1.8 was applied, as done for Soreq Cave, Judea Hills, Israel (Grant et al., 2012) and Manot Cave, Upper Galilee, Israel (Yas'ur, 2013; Hershkovitz et al., 2015). See Supplementary material for further details.

3.3.2. Age model

For each stalagmite, two methods were used to create the age model: linear interpolation and, the open source R software based algorithm "StalAge" (Scholz and Hoffmann, 2011). StalAge age models were used to identify major outliers and to provide an error envelope at 95% confidence limits. In addition, linearly interpolated age models were constructed using all ages in stratigraphic order and assuming continuous growth between two dated points. Sections of stalagmites in which the growth rates were substantially low compared with the rest of the sample were examined for evidence of hiatuses using petrographic criteria and sharp variations in isotopic composition. In cases where an indication for a hiatus was found, the sample was subdivided at the hiatus boundary into separate growth phases, and new linear interpolation and StalAge age models were constructed for the subsections. This subdivision created subsections in some of the samples for which age modelling using StalAge was not possible, either because they were only dated by less than three ages, or changes in growth rate within the section led to problems in the algorithm's check for outliers. In such cases, linearly interpolated age models were constructed for these sections of the samples, and usually were within the 95% confidence limit of the initial StalAge age models that did not account for hiatuses. Supplementary Figs. S3–S8 show the final age model compared with StalAge age models for each of the samples (Further detail is given in section 8.3 of the supplementary material). Where possible, $\delta^{18}O$ and $\delta^{13}C$ profiles from Zalmon Cave were also compared and fitted (within the 95% confidence limit) to the well dated $\delta^{18}O$ and $\delta^{13}C$ profiles of Soreq Cave (Kagan et al., 2005). This was done for the top portion of ZAL2 which has uncorrected ages of ~7.5 to ~6 ka and corrected ages of ~6.9 to ~5.1 ka, was slightly fitted to match the $\delta^{18}O$ profiles of ZAL6 (which were better constrained than ZAL2 with lower age errors and slower growth rate) and Soreq Cave speleothems (Fig. S9). These modifications deviate from corrected ages by less than 0.3 ka, well within the measurement error. Wiggle-matching with Soreq profile was also done for ZAL6. A hiatus was identified by the age gap determined for ZAL 6E (~19 ka) and ZAL 6D (~13 ka) which is supported by petrographic criteria (Fig. S2 F). Based on the best fit to Soreq isotopic profile we estimated the hiatus to last between 15 ka and 13.2 ka (Fig. S9). This procedure of "wiggle matching" is justified by the fact that speleothems from northern, central and "rain shadow" desert show very similar isotopic values and trends (Bar-Matthews et al., 2003; Vaks et al., 2003).

3.4. Checking for deposition in isotopic equilibrium

To verify whether speleothems from Zalmon Cave were deposited in isotopic equilibrium four laminae from three different stalagmites were measured and checked according to Hendy (1971) criteria (Fig. 2 and Fig. S2). A "replication test" (Bar-Matthews et al., 1997; Dorale et al., 2002; Dorale and Liu, 2009) was also performed by comparing between two growth laminae of the same age but from different speleothems, to see if they give similar isotopic profiles.

3.5. Stable isotope compositions of speleothems

For the purpose of constructing oxygen ($\delta^{18}O$) and carbon ($\delta^{13}C$) isotopic profiles laminae were sampled using a 0.8 mm diamond drill along the stalagmite growth axis, at between 13 and 17 drill holes per cm. 350 μg from each sampled drill hole was placed at the bottom of a clean vacuum vessel positioned horizontally and a few drops of 100% phosphoric acid (H_3PO_4) were added at the top. The vessel was then flushed with pure Helium for 10 min in order to remove atmospheric CO_2. After flushing, the sample and acid were allowed to interact, releasing CO_2 into the sealed vessel. Oxygen and carbon isotopes were measured using a Finnigan Gas Bench II extraction system attached to a ThermoFinnigan Delta PLUS XP continuous flow mass spectrometer. A Carrara Marble standard ($\delta^{13}C = 4.74‰$, $\delta^{18}O = -3.85‰$) was measured every 8 samples. All $\delta^{18}O$ and $\delta^{13}C$ values obtained were calibrated against the internal lab standard which was calibrated against the international standards NBS-19 and NBS-18, and reported in per-mil (‰) relative to the VPDB standard (Craig, 1957). Analytical reproducibility is better than 0.1‰ for both $\delta^{18}O$ and $\delta^{13}C$. In the absence of multiple-point normalization real accuracies of stable isotope data may exceed the measured reproducibility's.

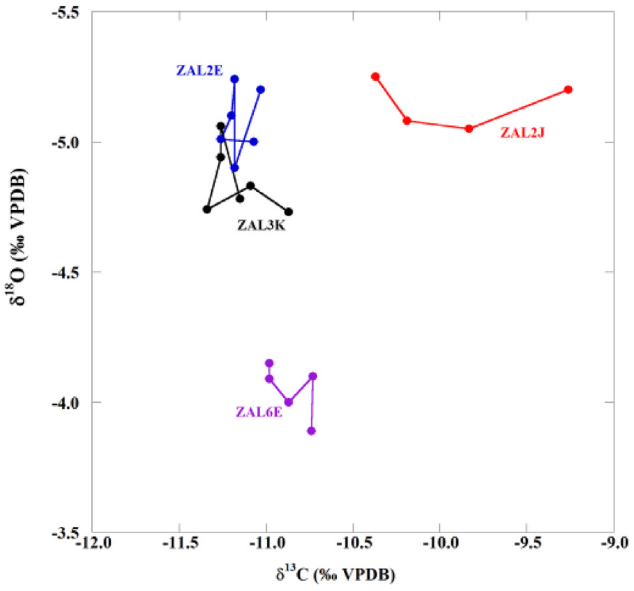

Fig. 2. $\delta^{18}O$ vs $\delta^{13}C$ along 4 representative laminae from samples ZAL2, ZAL3, and ZAL6 (see Fig. S2 for laminae location). $\delta^{18}O$ values throughout the laminae, show a maximum variation of 0.4‰. Changes of $\delta^{13}C$ do not correlate with changes of $\delta^{18}O$.

4. Results and discussion

4.1. Studied samples

A total of eight speleothems were collected in Zalmon Cave. ZAL1, 2, 3, 4 were found broken and their original location in the cave is not known. ZAL5, 6, 7 and 11 were removed in-situ (Fig. S1).

Three of these speleothems (ZAL2, ZAL3, and ZAL6) were used for reconstructing composite stable isotopic profiles over the last 70 ka where the highest age and spatial resolution was possible. The remaining five speleothems (ZAL1, ZAL4, ZAL5, ZAL7, and ZAL11) were used only to determine growth periods during MIS5 and MIS6 (Fig. 3, and Tables S1–S7); a detailed description of their petrography is given in supplemental material Section 8.1 and Fig. S2.

4.2. Deposition in isotopic equilibrium

Four laminae from three different stalagmites were sampled in various locations to determine if the speleothems were formed in isotopic equilibrium according to Hendy (1971) criteria (Fig. 2). In every lamina $\delta^{13}C$ variations do not correlate with those of $\delta^{18}O$, which only slightly change along the lamina with maximum difference of 0.4‰. Moreover, isotopic composition of speleothems that were deposited during the same time interval show similarities (Figs. S9–11) satisfying the "replication test" (Bar-Matthews et al., 1997; Dorale and Liu, 2009). These tests indicate that kinetic fractionation effects are negligible and that the speleothems from Zalmon Cave are suitable for paleoclimate reconstruction.

4.3. Dating results

The cumulative ages during the last 175 ka of all samples are presented in Fig. 3. For the full dating information, age corrections and age models of individual stalagmites refer to Sections 8.2, 8.3 and 8.4 and Table S8 of the supplementary material.

4.4. Growth periods

Deposition in Zalmon Cave was mostly continuous both during glacial and interglacial periods (Figs. 3 and 4) with few short intervals with no dated samples between 128-121 ka, 50-42 ka, 15-13 ka and 5-0 ka. Such depositional gaps most probably reflect lack of sampling, as was assumed for Peqi'in Cave (Bar-Matthews et al., 2003). Deposition of speleothems during interglacial periods indicates that the northern segment of the DSRV, the Eastern Galilee received an average annual rainfall of at least 300 mm as proposed for the Negev Desert (Vaks et al., 2006), central and northern Israel (Bar-Matthews et al., 2003). The almost continuous deposition is in contrast to speleothem growth in caves located along the central and southern DSRV (Fig. 1), which occurred primarily in glacial periods (Vaks et al., 2003; Lisker et al., 2010).

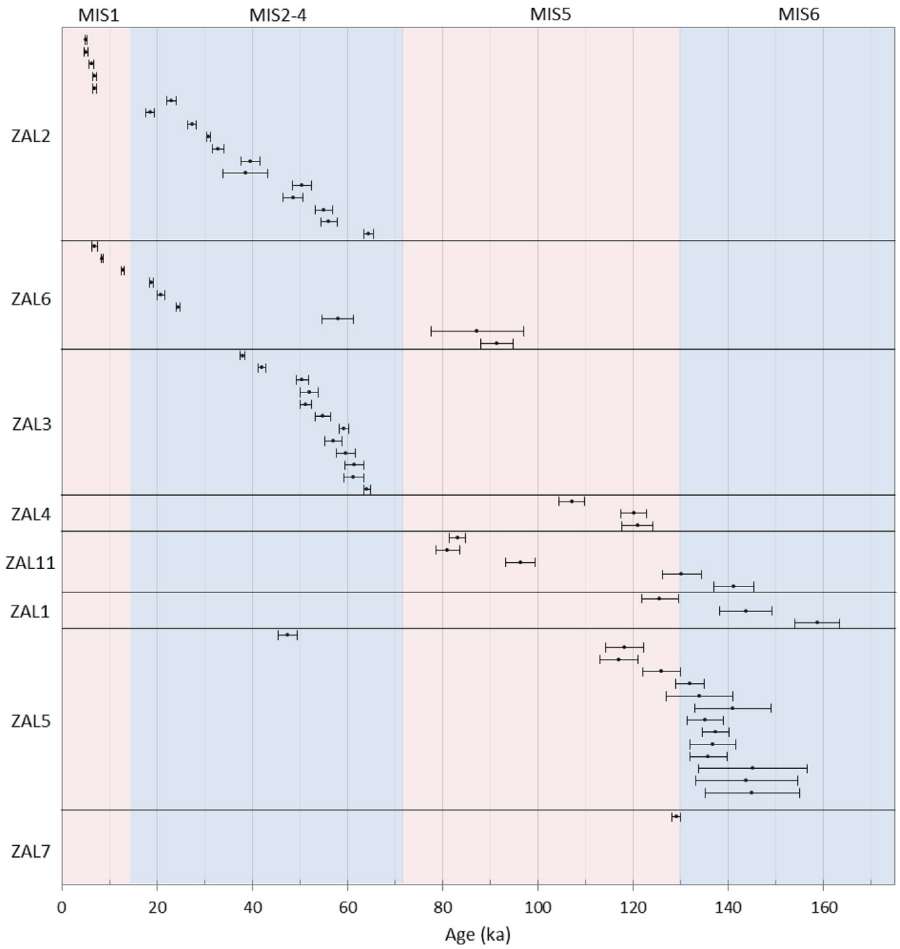

Fig. 3. Ages of stalagmites from Zalmon Cave with 2σ error bars. Discarded ages are not shown. Light blue/pink fields represent glacial/interglacial periods. Marine isotope stages (MIS) marked at the top of the diagram are after Lisiecki and Raymo (2005). (For interpretation of the references to colour in this figure legend, the reader is referred to the Web version of this article.)

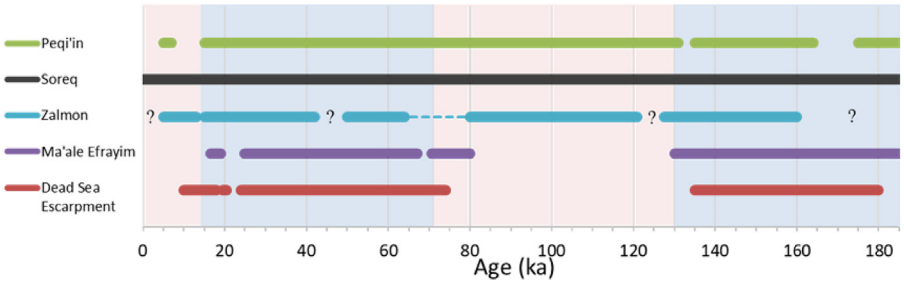

Fig. 4. Periods of speleothem deposition from various caves in the DSRV region. Light blue/pink fields represent glacial/interglacial periods (Lisiecki and Raymo, 2005). For Zalmon Cave, dashed line represents depositional periods with age reversals. (For interpretation of the references to colour in this figure legend, the reader is referred to the Web version of this article.)

It is clear that the growth pattern gradually changes from south to north along the DSRV. The southern segment exhibits very minimal growth limited only to glacial periods (Lisker et al., 2010). The central segment exhibits higher glacial deposition rates with limited interglacial deposition (Vaks et al., 2003), whereas results from this study show that the northern DSRV exhibits continuous growth for longer time intervals, throughout most of the interglacial and glacial periods. This suggests more rainfall in the northern part of the DSRV compared to its southern parts, similar to present-day conditions.

It is most probable that during the time interval of speleothems deposition in Zalmon Cave, the main source of precipitation to the northern DSRV is associated with a moisture source from the Eastern Mediterranean Sea, similar to central and northern Israel (Bar-Matthews et al., 2003). This source also contributes 90% of the rainfall today (Saaroni et al., 2010).

4.5. Isotopic composition of speleothems from Zalmon Cave and their paleoclimate significance

The high resolution stable isotopic record of Zalmon Cave speleothems during the Last Glacial MIS 4-2, between 71 and 14 ka forms the main focus of the study. This time interval is the time period when the precursor of the Dead Sea, Lake Lisan was in its higher stands (e.g., Torfstein et al., 2013).

A total of 558 samples from three different stalagmites (ZAL2, ZAL3, and ZAL6) were drilled for stable isotope measurements. All isotopic data and age models are given in section 8.4 and Tables S1–S7 in the supplementary material.

The composite isotopic profiles are plotted as black dots in Fig. 5 using the combined data from all samples (Table S8). Data are connected by an eight-point running average. Where two or more speleothems cover the same interval (e.g. ZAL2 and ZAL3 from 65 to 49 ka), the sample with higher resolution was chosen to be displayed. $\delta^{18}O$ values of Zalmon Cave speleothems vary between −6.4 and −3.7‰ with most values ranging between −5.6 and −4.3‰. $\delta^{13}C$ values vary between −13.2 and −8‰ with most values ranging between −11.3 and −9.7‰.

To appreciate the paleoclimate of the region in its wider context, the isotopic composition of Zalmon speleothems is compared with speleothems located in northern and central Israel (Peqi'in and Soreq caves speleothems, Bar-Matthews et al., 2003; Grant et al.,

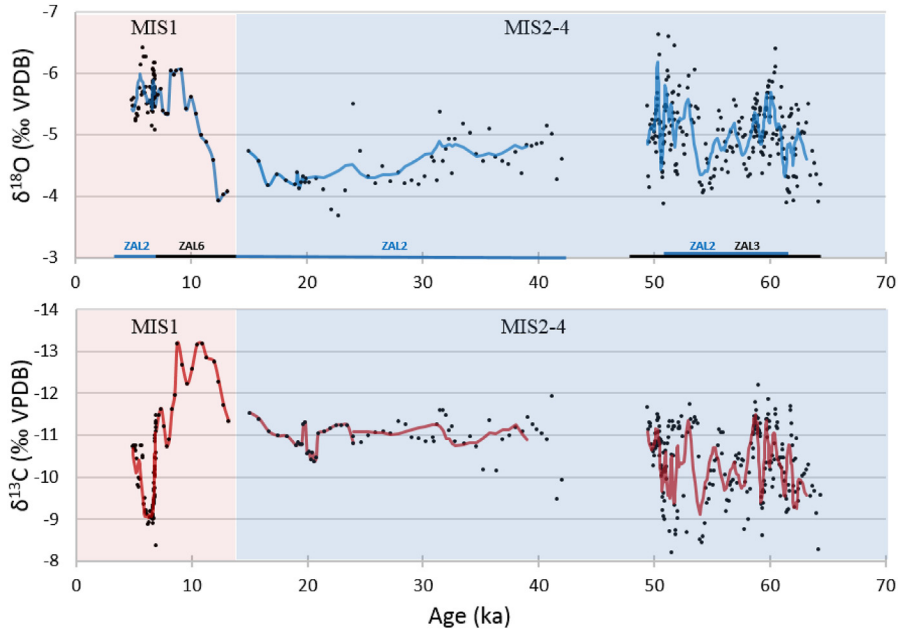

Fig. 5. Composite isotopic record from Zalmon Cave speleothems. Pink shaded areas define the Interglacial (MIS1) period and blue shaded areas the Last Glacial Period (MIS2-4). Eight point running average $\delta^{18}O$ and $\delta^{13}C$ values are plotted as blue and red lines, respectively. The samples used for the composite profile are shown at the bottom of $\delta^{18}O$ profile. (For interpretation of the references to colour in this figure legend, the reader is referred to the Web version of this article.)

2012) and with the isotopic composition of speleothems located in the central segment of the DSRV in the "rain-shadow" desert (Ma'ale Efrayim Cave, Vaks et al., 2003) (Fig. 6A and B). During most of the last glacial, $\delta^{18}O$ values in Zalmon Cave are ~0.5–1.0‰ lower than Peqi'in and Ma'ale Efrayim caves (Fig. 6A) and ~1–1.5‰ lower than Soreq Cave (Fig. 6B).

We interpret the data to indicate that local climate conditions in Zalmon Cave area are the main reasons for these depletions. The lower $\delta^{18}O$ of Zalmon Cave relative to Peqi'in Cave can largely be explained by higher temperature in the northern DSRV compared to Peqi'in Cave. Under present-day conditions the mean annual temperature in Peqi'in Cave area is 16 °C (Bar-Matthews et al., 2003), approximately 5 °C cooler than in the Zalmon Cave area.

In the case of the bigger $\delta^{18}O$ depletion of Zalmon Cave speleothems relative to Soreq and Ma'ale Efrayim Cave speleothems (Fig. 6A and B), we examine the possibility that the depletion trend of Zalmon Cave speleothems is caused by combination of increased temperature and Rayleigh distillation as storm tracks moved northeast from the Mediterranean coastline. First we examine the possibility that temperature difference alone (i.e. there was no difference in $\delta^{18}O$ water) during the last glacial period, could explain the $\delta^{18}O$ offset between the two cave speleothems. A 1‰ shift in $\delta^{18}O$ for carbonate precipitated in equilibrium would correspond to a temperature change of about 4 °C (O'Neil et al., 1969) meaning that the temperature at Zalmon Cave would have been 4–6 °C higher than Soreq Cave during the last glacial. However, clumped isotopes thermometry, fluid inclusion studies and sea surface temperatures (SST) studies (McGarry et al., 2004; Affek et al., 2008; Almogi-Labin et al., 2009) also indicate that the temperature in Soreq Cave was 6–10 °C colder than today during the LGM (where the $\delta^{18}O$ offset is 1.5‰) and 3 °C colder during a warm period at 56 ka (when the $\delta^{18}O$ offset is ~1‰). Similar observations of temperature differences have been interpreted for Mizpe Shelagim Cave in the north east (Ayalon et al., 2013). Thus, if glacial temperatures in Zalmon Cave region were indeed 4–6 °C higher than Soreq Cave, this would imply that the temperature was similar to present-day during the last glacial period. Such temperatures are not in line with calculated SST, and temperatures based on clumped

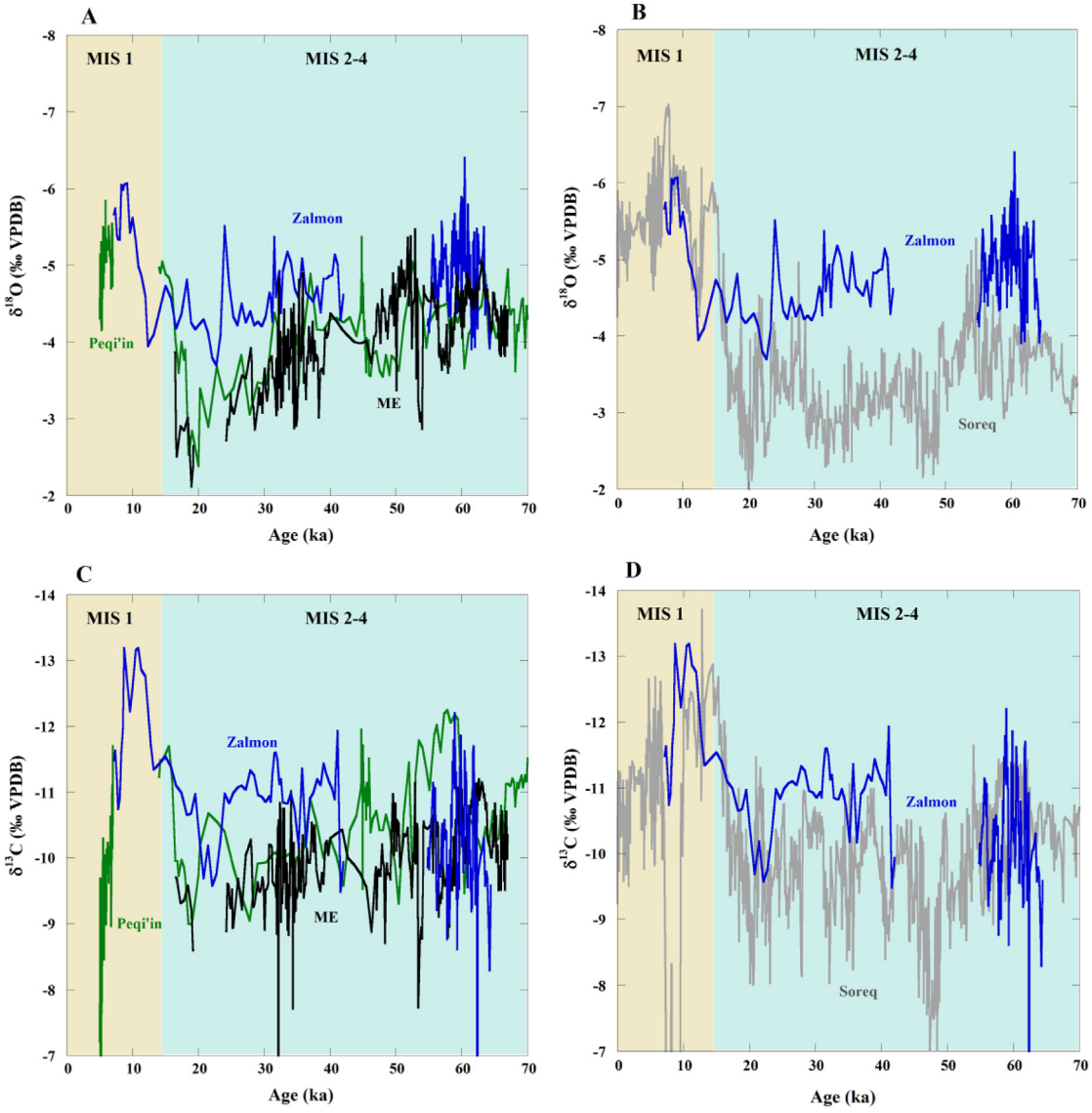

Fig. 6. Comparison of the Zalmon Cave $\delta^{18}O$ composite record with (A) Peqi'in Cave (Bar-Matthews et al., 2003), Ma'ale Efrayim Cave (ME) (Vaks et al., 2003): (B) with Soreq Cave (Grant et al., 2012). (C) and (D) show the comparison of Zalmon Cave $\delta^{13}C$ composite record with for the same caves. Line colours: Zalmon Cave (Blue), Peqi'in Cave (Green), Ma'ale Efrayim Cave (ME) (Black), Soreq Cave (light Grey). (For interpretation of the references to colour in this figure legend, the reader is referred to the Web version of this article.)

isotopes and fluid inclusions from Soreq, Ma'ale Efrayim, and Mizpe Shelagim caves area (McGarry et al., 2004; Affek et al., 2008; Almogi-Labin et al., 2009; Ayalon et al., 2013). It is important to note that in present-day conditions data from Israel Meteorological Service stations show that the average annual temperature and precipitation in Zalmon Cave area is 21 ± 0.5 °C and 550 mm, respectively, similar to Soreq Cave area values (20.5 °C and 500 mm). It follows that temperature difference alone cannot fully explain the depleted Zalmon $\delta^{18}O$ values. It is thus more likely that the depletion was a result of combined increased temperature and Rayleigh distillation isotopic depletion effects as the storm tracks travelled inland from the sea.

$\delta^{13}C$ values of Zalmon Cave speleothems range between ~ -11.5 and −10.5‰, indicating that C3 vegetation dominated the cave's region throughout the last glacial, implying relatively humid conditions (Fig. 5). These $\delta^{13}C$ values are similar to those of Peqi'in Cave, but are significantly lower, mostly during the time interval younger than ~55 ka than those of Soreq and Ma'ale Efrayim caves speleothems (Fig. 6C and D). Higher $\delta^{13}C$ values in Soreq and Ma'ale Efrayim speleothems reflect higher proportion of C4 plant and/or stress condition for C3 plant vegetation (e.g., Bar-Matthews et al., 2003) suggesting that Zalmon Cave area was much more humid during larger part of the last glacial. Thus, an alternative scenario to explain the depletion of $\delta^{18}O$ values of Zalmon Cave speleothems is higher input of rainfall in the cave region compared to central Israel and central DSRV during the last glacial.

An enhanced rainfall scenario is at first sight in contradiction to the notion that Rayleigh isotopic depletion occurred as a result of eastward direct rainout. Thus, in order to explain the enhanced rainfall scenario in Zalmon Cave area a different moisture trajectory for the last glacial period is examined, as suggested by Enzel et al. (2008) and Goldsmith et al. (2016). Presently, the main contributors of rainfall in Israel, imparting 90% of the annual amount, are cyclones known as Cyprus lows (storms passing, intensifying or even developing over Cyprus). These storms transport cool air originating from Eastern Europe over the warmer Mediterranean, where it becomes moist and unstable (Saaroni et al., 2010). Enzel et al. (2008) proposed that during the last glacial, the Eastern Mediterranean cyclones were deflected southwards (Fig. 7) by the snow covered European and Turkish landmasses and lowered sea level, leading to storm tracks being funneled along the Mediterranean Sea directly eastward to the Levant. This trajectory could have enhanced rainfall in the northern DSRV catchment area while central Israel would have received roughly the same amounts. Based on the Yammoûneh sequence (Develle et al., 2010, 2011), these proposed last glacial westerlies systems did not penetrate as far north as the northern Levant.

Examination of the bathymetry of the Eastern Mediterranean shows that during the LGM the coastline regression opposite south and central Israel was ~20 km farther than that of northern Israel and Lebanon (Hall et al., 1994) (Fig. 7). With present-day synoptic systems, Rayleigh effects resulting from the longer distance from the source waters (and higher elevation ~120 m) should bring about lower $\delta^{18}O$ values in Soreq Cave speleothems, rather than at Zalmon Cave. This implies that the relative distance effects were negligible and/or the storm tracks travelled a longer distance to Zalmon Cave's location, consistent with the southern shift in the synoptic system.

Interestingly, the largest shifts towards relatively lower $\delta^{18}O$ and $\delta^{13}C$ values in Zalmon Cave speleothems occurred during last glacial (Fig. 6) and coincide with the highest stand of Lake Lisan in the DSRV (Fig. 8F). Stein et al. (1997) argue that the high lake stands occurred at periods of relatively increased moisture and increased fresh water input in the lake catchment area. Enzel et al. (2008) suggested that the lake levels were directly influenced by

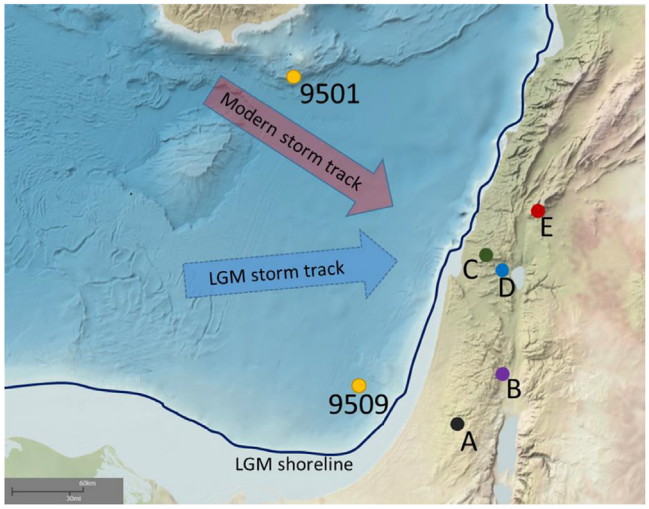

Fig. 7. Bathymetric map of the Eastern Mediterranean Sea (NOAA – National Oceanic and Atmospheric Administration) with estimated last glacial maximum (LGM) shoreline as a dark blue line. Modern day wind directions as a pink arrow. Proposed last glacial period wind direction as a blue arrow (Enzel et al., 2008). Cave locations represented by capital letters: A - Soreq, B - Ma'ale Efrayim, C – Peqi'in, D - Zalmon, E – Mizpe Shelagim. Marine core 9501 and 9509 locations as yellow circles (modified from Almogi-Labin et al., 2009). (For interpretation of the references to colour in this figure legend, the reader is referred to the Web version of this article.)

regional climate in the Eastern Mediterranean during the late Pleistocene. Torfstein et al. (2013) argue that evaporation rates during the glacial period were as high as or possibly higher than present-day, thus emphasizing the requirement for significant increased freshwater input as the source of the lake level high stands. These studies concluded that lake level fluctuations are overwhelmingly controlled by the precipitation component of the regional hydrological cycle. However, there are additional processes that could help bring about high lake levels. Lake Lisan's high stands are associated with high precipitation/evaporation ratios, which possibly resulted from lower temperatures during the last glacial and more effective water infiltration (Bar-Matthews et al., 1997, 2003; Vaks et al., 2003, 2006). Ayalon et al. (2013) also noted that significant snow melting during short warm periods in the last glacial, would have resulted in increased water drainage from Mt. Hermon and probably other high elevation sites in the region, which flowed down to the Jordan River towards Lake Lisan.

To conclude, the low Zalmon Cave $\delta^{18}O$ values observed during the last glacial period most likely imply that the cave's region was humid. This assumption is further supported by the slightly lower $\delta^{13}C$ values implying the dominance of C3 type vegetation, which is indicative to humid climate. A probable explanation for the offset between Soreq and Zalmon caves can be explained by a combination of a significantly larger amount of rainfall associated with a different synoptic system and, possibly, a slight temperature difference (no more than 1–2 °C).

4.6. The source effect variations

$\delta^{18}O$ values of cave drips reflect the $\delta^{18}O$ of rainwater from which speleothems were deposited, thus speleothems' $\delta^{18}O$ variations mainly reflect changes in sea surface source (Frumkin et al., 1999) of atmospheric vapor that leads to cloud formation. $\Delta\delta^{18}O$, defined as the difference between the marine sea surface source and rainfall, results from a complex combination of evaporation processes above the sea, distance travelled by the clouds over land, cooling effects due to increased elevation, and the “amount effect”.

Bar-Matthews et al. (2003) showed that in the Eastern Mediterranean the average $\Delta\delta^{18}O_{sea-land}$ values, documented by the difference between Soreq Cave speleothems $\delta^{18}O$ and the planktonic foraminifera *Globigerinoides ruber* $\delta^{18}O$ values, is relatively constant at 5.6 ± 0.7‰ during the last 185 ka and oscillations in $\Delta\delta^{18}O$ largely reflect the amount effect. Kolodny et al. (2005) interpreted this relative constancy across the last glacial–present interglacial transition to indicate that the Easterm Mediterranean speleothems $\delta^{18}O$ record primarily reflects sea surface $\delta^{18}O$ changes.

The isotopic records of Zalmon Cave as well as speleothem records from Peqi'in and Ma'ale Efrayim caves are compared to the $\delta^{18}O$ values of the planktonic foraminifera *G. ruber* from marine cores 9501 and 9509 (Fig. 1) as previously was done by Almogi-Labin et al. (2009) for Soreq Cave speleothems (Fig. 8). The differences are presented as a three point moving averages (Fig. 8A–D). During the last glacial period coinciding with peak Lake Lisan levels ~25–35 ka (Fig. 8F), Zalmon Cave's $\Delta\delta^{18}O_{sea-speleothems}$ values varied between 5 and 9‰ (Fig. 8D), consistently higher than those of Soreq, Peqi'in and Ma'ale Efrayim caves during last glacial (Figs. 8 and 9). The $\Delta\delta^{18}O_{sea-speleothems}$ differences are generally smaller

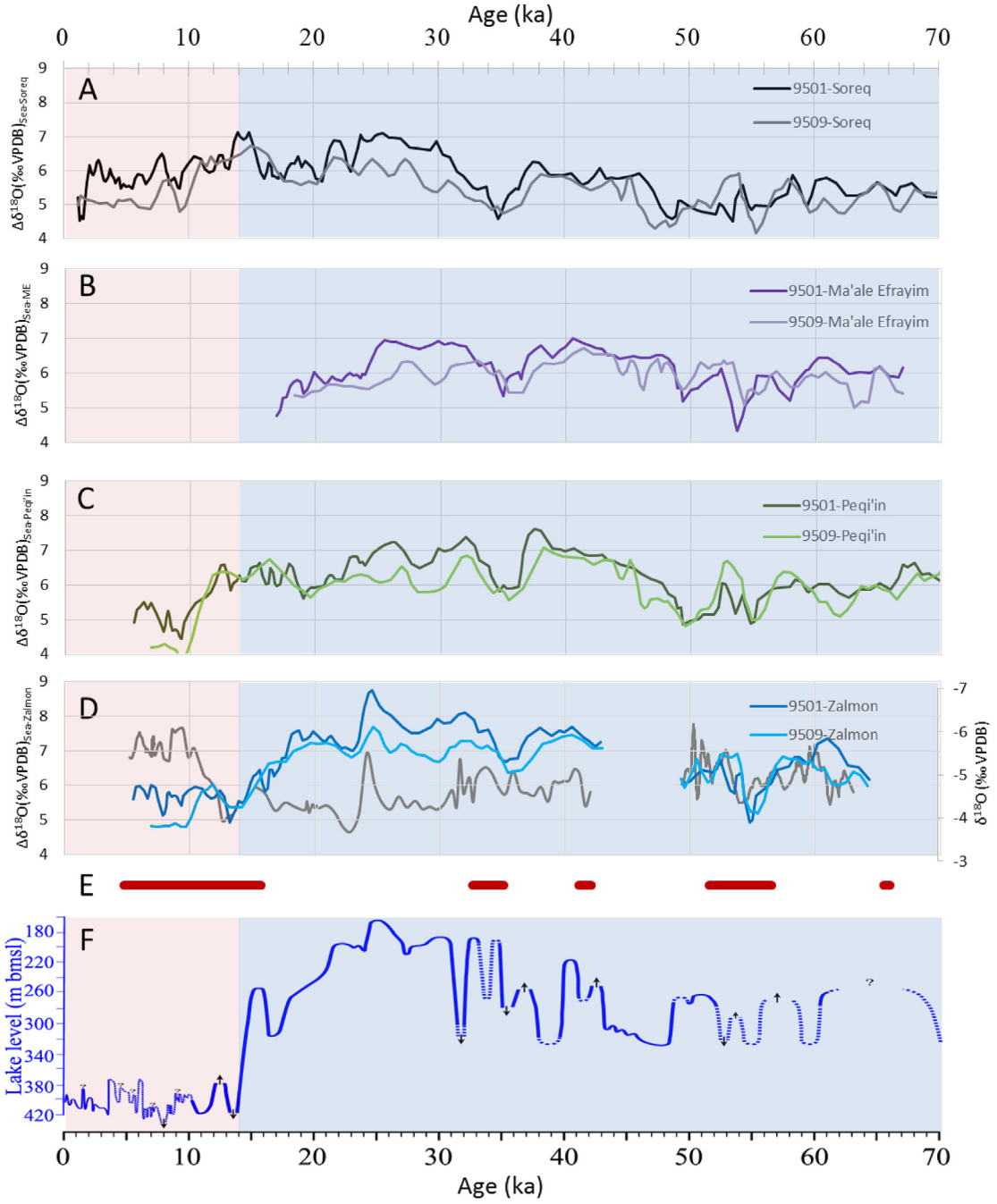

Fig. 8. A-D Comparisons between $\delta^{18}O_{G.ruber}$ (Almogi-Labin et al., 2009) and $\delta^{18}O_{land(cave)}$ records plotted as $\Delta\delta^{18}O_{sea-land}$ values; Dark lines - $\Delta\delta^{18}O_{9501-cave}$. Light lines - $\Delta\delta^{18}O_{9509-cave}$. Marine core 9501 is was taken offshore of the northern Levant, whereas core 9509 was taken offshore of the Southern Levant (Fig. 1A). The curves in A-D are generated using three point moving averages. A - $\Delta\delta^{18}O_{sea(9501\ \&\ 9509)-Soreq}$. B - $\Delta\delta^{18}O_{sea-Ma'ale\ Efrayim}$. C - $\Delta\delta^{18}O_{sea-Peqi'in}$. D - $\Delta\delta^{18}O_{sea-Zalmon}$. Zalmon Cave $\delta^{18}O$ as a grey line. E – Deposition periods in Mizpe Shelagim Cave attributed to short warming periods within the last glacial period (Ayalon et al., 2013). F - Lake Lisan lake level curve modified after Torfstein et al. (2013).

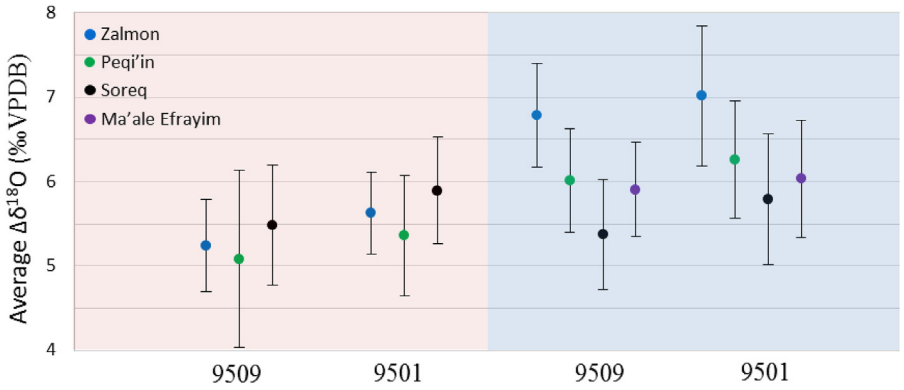

Fig. 9. Average $\Delta\delta^{18}O_{sea\text{-}cave}$ values for MIS1 (pink) and the last glacial period (light blue). Standard deviation as black error bars. Average $\Delta\delta^{18}O_{sea\text{-}Soreq}$ are similar for both MIS1 and the last glacial. Average glacial $\Delta\delta^{18}O_{sea\text{-}Peqi'in}$ is ~1‰ higher than during MIS1. Average glacial $\Delta\delta^{18}O_{sea\text{-}Zalmon\ is}$ ~1.5‰ higher than during MIS1. $\Delta\delta^{18}O_{9509\text{-}land}$ values are consistently lower than $\Delta\delta^{18}O_{9501\text{-}cave}$ for all 4 caves and both time periods. (For interpretation of the references to colour in this figure legend, the reader is referred to the Web version of this article.)

during warm periods, and coincide with deposition of speleothems in Mizpe Shelagim Cave. The higher $\Delta\delta^{18}O_{sea\text{-}Zalmon}$ values during last glacial indicate that $\delta^{18}O$ values from Zalmon Cave speleothems deviate from the "source effect" much more than the other caves. Why is the "source effect" less pronounced in Zalmon Cave? Can the southern shift of the glacial storm tracks explain this deviation? A possible scenario is an increase in rainfall in Zalmon cave area, resulting in lower $\delta^{18}O$ due to "amount effect". Indeed, the proposed southward shifts of the storm direction during the last glacial period (Enzel et al., 2008) accord with the proposed wind directions (Fig. 7), implying more rainfall in the northern DSRV relative to central and northern Israel, and resulting in higher $\Delta\delta^{18}O_{sea\text{-}Zalmon}$ differences.

5. Conclusions

Growth periods and isotopic composition of speleothems from the newly discovered Zalmon Cave, located in the northern segment of the DSRV, on the boundary between Mediterranean climate region and the 'rain-shadow' desert region, offer a new insight into the hydrological conditions of the DSRV during last glacial. Speleothems from the Mediterranean climate zone grew continuously throughout several glacial/interglacial cycles, indicating that water was always available in the unsaturated zone. Their $\delta^{18}O$ variations match global and regional climate changes, with the Eastern Mediterranean Sea being the major control on their $\delta^{18}O$ values, as evident from the similarity between the speleothems and the planktonic foraminifer *G. ruber* records. However, unlike speleothems from central and the southern DSRV, Zalmon Cave speleothems grew both during glacial and interglacial periods, as in the Mediterranean climate region. Nevertheless, during last glacial their $\delta^{18}O$ values were shifted to lower values by ~1–2‰ relative to speleothems from central Israel (Soreq Cave). The largest difference in $\delta^{18}O$ values between Zalmon Cave speleothems and *G. ruber* from offshore marine cores also occurred during most of the last glacial period. The data are consistent with a suggested southward shift of the westerlies' storm tracks that occurred during this period, and resulted in increased rainfall in the northern DSRV, providing freshwater input during the otherwise relatively 'drier' glacial.

Acknowledgments

This research was supported by United States-Israel Binational Science Foundation grant number 2010316 to M.B.M. and DESERVE Virtual Institute of Helmholtz Association granted to A. Agnon. We would like to thank N. Tapliakov from the Geological Survey of Israel for her help in the laboratory work, Yaron Katzir and Bar Elisha from Ben-Gurion University for help with the petrographic thin sections. We would like to thank Alan Matthews, the two anonymous reviewers and the editors for critical review which significantly improved the manuscript.

Appendix A. Supplementary data

Supplementary data to this article can be found online at https://doi.org/10.1016/j.quascirev.2019.07.018.

References

NOAA – National Oceanic and atmospheric administartion, https://maps.ngdc.noaa.gov/viewers/bathymetry/.

Affek, H.P., Bar-Matthews, M., Ayalon, A., Matthews, A., Eiler, J.M., 2008. Glacial/interglacial temperature variations in Soreq cave speleothems as recorded by 'clumped isotope' thermometry. Geochem. Cosmochim. Acta 72, 5351–5360. https://doi.org/10.1016/j.gca.2008.06.031.

Almogi-Labin, A., Bar-Matthews, M., Shriki, D., Kolosovsky, E., Paterne, M., Schilman, B., Ayalon, A., Aizenshtat, Z., Matthews, A., 2009. Climatic variability during the last ~90ka of the southern and northern Levantine Basin as evident from marine records and speleothems. Quat. Sci. Rev. 28, 2882–2896. https://doi.org/10.1016/j.quascirev.2009.07.017.

Arkin, Y., Braun, M., Starinsky, A., Hamaoui, M., Raab, M., 1965. Type Sections of Cretaceous Formations in the Jerusalem Bet Semesh Area. Geological Survey of Israel.

Ayalon, A., Bar-Matthews, M., Kaufman, A., 2002. Climatic conditions during marine oxygen isotope stage 6 in the eastern Mediterranean region from the isotopic composition of speleothems of Soreq Cave, Israel. Geology 30, 303–306. https://doi.org/10.1130/0091-7613(2002)030<0303:CCDMOI>2.0.CO.

Ayalon, A., Bar-Matthews, M., Frumkin, A., Matthews, A., 2013. Last Glacial warm events on Mount Hermon: the southern extension of the Alpine karst range of the east Mediterranean. Quat. Sci. Rev. 59, 43–56. https://doi.org/10.1016/j.quascirev.2012.10.047.

Bar-Matthews, M., 2014. History of water in the Middle East and north Africa. In: Treatise on Geochemistry. Elsevier, pp. 109–128. https://doi.org/10.1016/B978-0-08-095975-7.01210-9.

Bar-Matthews, M., Ayalon, A., 2011. Mid-Holocene climate variations revealed by high-resolution speleothem records from Soreq Cave, Israel and their correlation with cultural changes. Holocene 21, 163–171. https://doi.org/10.1177/0959683610384165.

Bar-Matthews, M., Ayalon, A., Kaufman, A., 1997. Late quaternary paleoclimate in the eastern mediterranean region from stable isotope analysis of speleothems at Soreq cave, Israel. Quat. Res. 47, 155–168. https://doi.org/10.1006/qres.1997.1883.

Bar-Matthews, M., Ayalon, A., Kaufman, A., 2000. Timing and hydrological conditions of Sapropel events in the Eastern Mediterranean, as evident from speleothems, Soreq cave, Israel. Chem. Geol. 169, 145–156. https://doi.org/10.1016/S0009-2541(99)00232-6.

Bar-Matthews, M., Ayalon, A., Gilmour, M., Matthews, A., Hawkesworth, C.J., 2003. Sea–land oxygen isotopic relationships from planktonic foraminifera and

speleothems in the Eastern Mediterranean region and their implication for paleorainfall during interglacial intervals. Geochem. Cosmochim. Acta 67, 3181–3199. https://doi.org/10.1016/S0016-7037(02)01031-1.
Bar-Matthews, M., Ayalon, A., Vaks, A., Frumkin, A., 2017. Climate and environment reconstructions based on speleothems from the levant. In: Enzel, Y., Bar-Yosef, O. (Eds.), Quaternary of the Levant. Cambridge University Press, Cambridge, pp. 151–164. https://doi.org/10.1017/9781316106754.017.
Bartov, Y., Stein, M., Enzel, Y., Agnon, A., Reches, Z., 2002. lake levels and sequence stratigraphy of Lake Lisan, the late Pleistocene precursor of the Dead Sea. Quat. Res. 57, 9–21. https://doi.org/10.1006/qres.2001.2284.
Bogoch, R., Sneh, A., 2008. Geological Map of Israel, 1:50000 Israel Geological Survey (Sheet 4-1).
Cheng, H., Edwards, R., Hoff, J., Gallup, C., Richards, D., Asmerom, Y., 2000. The half-lives of uranium-234 and thorium-230. Chem. Geol. v. 169, 17–33. https://doi.org/10.1016/S0009-2541(99)00157-6.
Craig, H., 1957. Isotopic standards for carbon and oxygen and correction factors for mass-spectrometric analysis of carbon dioxide. Geochem. Cosmochim. Acta 12, 133–149. https://doi.org/10.1016/0016-7037(57)90024-8.
Develle, A.-L., Herreros, J., Vidal, L., Sursock, A., Gasse, F., 2010. Controlling factors on a paleo-lake oxygen isotope record (Yammoûneh, Lebanon) since the Last Glacial Maximum. Quat. Sci. Rev. 29, 865–886. https://doi.org/10.1016/j.quascirev.2009.12.005.
Develle, A.-L., Gasse, F., Vidal, L., Williamson, D., Demory, F., Van Campo, E., Ghaleb, B., Thouveny, N., 2011. A 250ka sedimentary record from a small karstic lake in the Northern Levant (Yammoûneh, Lebanon). Palaeogeogr. Palaeoclimatol. Palaeoecol. v. 305, 10–27. https://doi.org/10.1016/j.palaeo.2011.02.008.
Dorale, J.A., Liu, Z., 2009. Limitations of hendy test criteria in judging the paleoclimatic suitability of speleothems and the need for replication. J. Cave Karst Stud. 71, 73–80 doi: PNR61.
Dorale, J.A., Edwards, R.L., Onac, B.F., 2002. Final Report of IGCP379. In: Daoxian, Y., Cheng, Z. (Eds.), Karst Processes and the Carbon Cycle.
Enzel, Y., Amit, R., Dayan, U., Crouvi, O., Kahana, R., Ziv, B., Sharon, D., 2008. The climatic and physiographic controls of the eastern Mediterranean over the late Pleistocene climates in the southern Levant and its neighboring deserts. Glob. Planet. Chang. 60, 165–192. https://doi.org/10.1016/j.gloplacha.2007.02.003.
Fleitmann, D., Burns, S.J., Mudelsee, M., Neff, U., Kramers, J., Mangini, A., Matter, A., 2003a. Holocene forcing of the Indian monsoon recorded in a stalagmite from southern Oman. Science 300, 1737–1739.
Fleitmann, D., Burns, S.J., Neff, U., Mangini, A., Matter, A., 2003b. Changing moisture sources over the last 330,000 years in Northern Oman from fluid-inclusion evidence in speleothems. Quat. Res. 60, 223–232. https://doi.org/10.1016/S0033-5894(03)00086-3.
Fleitmann, D., Burns, S.J., Pekala, M., Mangini, A., Al-Subbary, A., Al-Aowah, M., Kramers, J., Matter, A., 2011. Holocene and Pleistocene pluvial periods in Yemen, southern Arabia. Quat. Sci. Rev. 30, 783–787. https://doi.org/10.1016/j.quascirev.2011.01.004.
Frisia, S., 2015. Microstratigraphic logging of calcite fabrics in speleothems as tool for palaeoclimate studies. Int. J. Speleol. 44, 1–16. https://doi.org/10.5038/1827-806X.44.1.1.
Frumkin, A., Fischhendler, I., 2005. Morphometry and distribution of isolated caves as a guide for phreatic and confined paleohydrological conditions. Geomorphology 67, 457–471. https://doi.org/10.1016/j.geomorph.2004.11.009.
Frumkin, A., Ford, D.C., Schwarcz, H.P., 1999. Continental oxygen isotopic record of the last 170,000 Years in Jerusalem. Quat. Res. 51, 317–327. https://doi.org/10.1006/qres.1998.2031.
Gasse, F., Vidal, L., Van Campo, E., Demory, F., Develle, A.-L., Tachikawa, K., Elias, A., Bard, E., Garcia, M., Sonzogni, C., Thouveny, N., 2015. Hydroclimatic changes in northern Levant over the past 400,000 years. Quat. Sci. Rev. 111, 1–8. https://doi.org/10.1016/j.quascirev.2014.12.019.
Goldsmith, Y., Polissar, P.J., Ayalon, A., Bar-Matthews, M., DeMenocal, P.B., Broecker, W.S., 2016. The modern and Last Glacial Maximum hydrological cycles of the Eastern Mediterranean and the Levant from a water isotope perspective. Earth Planet. Sci. Lett. https://doi.org/10.1016/j.epsl.2016.10.017.
Grant, K.M., Rohling, E.J., Bar-Matthews, M., Ayalon, A., Medina-Elizalde, M., Ramsey, C.B., Satow, C., Roberts, A.P., 2012. Rapid coupling between ice volume and polar temperature over the past 150,000 years. Nature 491, 744–747. https://doi.org/10.1038/nature11593.
Hall, J.K., Udintsev, G.B., Odinikov, Y.Y., 1994. The Bottom Relief of the Levantine Sea: Geologic Structure of the Northeastern Mediterranean: Jerusalem. Historical Productions-Hall Ltd., pp. 5–32
Hendy, C., 1971. The isotopic geochemistry of speleothems—I. The calculation of the effects of different modes of formation on the isotopic composition of speleothems and their applicability as palaeoclimatic indicators. Geochem. Cosmochim. Acta 35, 801–824. https://doi.org/10.1016/0016-7037(71)90127-X.
Hershkovitz, I., Marder, O., Ayalon, A., Bar-Matthews, M., Yasur, G., Boaretto, E., Caracuta, V., Alex, B., Frumkin, A., Goder-Goldberger, M., Gunz, P., Holloway, R.L., Latimer, B., Lavi, R., et al., 2015. Levantine cranium from Manot Cave (Israel) foreshadows the first European modern humans. Nature 520, 216–219. https://doi.org/10.1038/nature14134.
IMS - Israel Meteorological Service, 2011. Average annual precipitation map 1981-2010. http://www.ims.gov.il/IMS/CLIMATE/ClimaticAtlas/RainMaps.htm, 1.
Kagan, E.J., Agnon, A., Bar-Matthews, M., Ayalon, A., 2005. Dating large infrequent earthquakes by damaged cave deposits. Geology 33, 261–264. https://doi.org/10.1130/G21193.1.
Kaufman, A., Wasserburg, G.J., Porcelli, D., Bar-Matthews, M., Ayalon, A., Halicz, L., 1998. U-Th isotope systematics from the Soreq cave, Israel and climatic correlations. Earth Planet. Sci. Lett. 156, 141–155. https://doi.org/10.1016/S0012-821X(98)00002-8.
Kolodny, Y., Stein, M., Machlus, M., 2005. Sea-rain-lake relation in the last glacial east mediterranean revealed by $\delta^{18}O$-$\delta^{13}C$ in Lake Lisan aragonites. Geochem. Cosmochim. Acta 69, 4045–4060. https://doi.org/10.1016/j.gca.2004.11.022.
Li, W.-X., Lundberg, J., Dickin, A.P., Ford, D.C., Schwarcz, H.P., McNutt, R., Williams, D., 1989. High-precision mass-spectrometric uranium-series dating of cave deposits and implications for palaeoclimate studies. Nature 339, 534–536. https://doi.org/10.1038/339534a0.
Lisiecki, L.E., Raymo, M.E., 2005. A Pliocene-Pleistocene stack of 57 globally distributed benthic δ18O records. Paleoceanography 20. https://doi.org/10.1029/2004PA001071.
Lisker, S., Vaks, A., Bar Matthews, M., Porat, R., Frumkin, A., 2010. Late Pleistocene palaeoclimatic and palaeoenvironmental reconstruction of the Dead Sea area (Israel), based on speleothems and cave stromatolites. Quat. Sci. Rev. 29, 1201–1211. https://doi.org/10.1016/j.quascirev.2010.01.018.
Litt, T., Pickarski, N., Heumann, G., Stockhecke, M., Tzedakis, P.C., 2014. A 600,000 year long continental pollen record from Lake Van, eastern Anatolia (Turkey). Quat. Sci. Rev. 104, 30–41. https://doi.org/10.1016/j.quascirev.2014.03.017.
McGarry, S., Bar-Matthews, M., Matthews, A., Vaks, A., Schilman, B., Ayalon, A., 2004. Constraints on hydrological and paleotemperature variations in the Eastern Mediterranean region in the last 140ka given by the δD values of speleothem fluid inclusions. Quat. Sci. Rev. 23, 919–934. https://doi.org/10.1016/j.quascirev.2003.06.020.
Nehme, C., Verheyden, S., Noble, S.R., Farrant, A.R., Sahy, D., Hellstrom, J., Delannoy, J.J., Claeys, P., 2015. Reconstruction of MIS 5 climate in the central Levant using a stalagmite from Kanaan Cave, Lebanon. Clim. Past 11, 1785–1799. https://doi.org/10.5194/cp-11-1785-2015.
O'Neil, J.R., Clayton, R.N., Mayeda, T.K., 1969. Oxygen isotope fractionation in divalent metal carbonates. J. Chem. Phys. 51, 5547. https://doi.org/10.1063/1.1671982.
Richards, D. a, Dorale, J. a, 2003. Uranium-series chronology and environmental applications of speleothems. Rev. Mineral. Geochem. 52, 407–460. https://doi.org/10.2113/0520407.
Rossignol-Strick, M., 1985. Mediterranean Quaternary sapropels, an immediate response of the African monsoon to variation of insolation. Palaeogeogr. Palaeoclimat. Palaeoecol. 49, 237–263. https://doi.org/10.1016/0031-0182(85)90056-2.
Saaroni, H., Halfon, N., Ziv, B., Alpert, P., Kutiel, H., 2010. Links between the rainfall regime in Israel and location and intensity of Cyprus lows. Int. J. Climatol. 30, 1014–1025. https://doi.org/10.1002/joc.1912.
Scholz, D., Hoffmann, D.L., 2011. StalAge – an algorithm designed for construction of speleothem age models. Quat. Geochronol. 6, 369–382. https://doi.org/10.1016/j.quageo.2011.02.002.
Shen, C.-C., Lawrence Edwards, R., Cheng, H., Dorale, J.A., Thomas, R.B., Bradley Moran, S., Weinstein, S.E., Edmonds, H.N., 2002. Uranium and thorium isotopic and concentration measurements by magnetic sector inductively coupled plasma mass spectrometry. Chem. Geol. 185, 165–178. https://doi.org/10.1016/S0009-2541(01)00404-1.
Stein, M., Starinsky, A., Katz, A., Goldstein, S.L., Machlus, M., Schramm, A., 1997. Strontium isotopic, chemical, and sedimentological evidence for the evolution of Lake Lisan and the Dead Sea. Geochem. Cosmochim. Acta 61, 3975–3992. https://doi.org/10.1016/S0016-7037(97)00191-9.
Stockhecke, M., Sturm, M., Brunner, I., Schmincke, H.-U., Sumita, M., Kipfer, R., Cukur, D., Kwiecien, O., Anselmetti, F.S., 2014. Sedimentary evolution and environmental history of Lake Van (Turkey) over the past 600 000 years. In: Ariztegui, D. (Ed.), Sedimentology, vol. 61, pp. 1830–1861. https://doi.org/10.1111/sed.12118.
Torfstein, A., Haase-Schramm, A., Waldmann, N., Kolodny, Y., Stein, M., 2009. U-series and oxygen isotope chronology of the mid-Pleistocene Lake Amora (Dead Sea basin). Geochem. Cosmochim. Acta 73, 2603–2630. https://doi.org/10.1016/j.gca.2009.02.010.
Torfstein, A., Goldstein, S.L., Stein, M., Enzel, Y., 2013. Impacts of abrupt climate changes in the levant from last glacial Dead Sea levels. Quat. Sci. Rev. 69, 1–7. https://doi.org/10.1016/j.quascirev.2013.02.015.
Vaks, A., Bar-Matthews, M., Ayalon, A., Schilman, B., Gilmour, M., Hawkesworth, C.J., Frumkin, A., Kaufman, A., Matthews, A., 2003. Paleoclimate reconstruction based on the timing of speleothem growth and oxygen and carbon isotope composition in a cave located in the rain shadow in Israel. Quat. Res. 59, 182–193. https://doi.org/10.1016/S0033-5894(03)00013-9.
Vaks, A., Bar-Matthews, M., Ayalon, A., Matthews, A., Frumkin, A., Dayan, U., Halicz, L., Almogi-Labin, A., Schilman, B., 2006. Paleoclimate and location of the border between Mediterranean climate region and the Saharo-Arabian Desert as revealed by speleothems from the northern Negev Desert, Israel. Earth Planet. Sci. Lett. 249, 384–399. https://doi.org/10.1016/j.epsl.2006.07.009.
Vaks, A., Bar-Matthews, M., Ayalon, A., Matthews, A., Halicz, L., Frumkin, A., 2007. Desert speleothems reveal climatic window for African exodus of early modern humans. Geology 35, 831–834. https://doi.org/10.1130/G23794A.1.
Vaks, A., Bar-Matthews, M., Matthews, A., Ayalon, A., Frumkin, A., 2010. Middle-late quaternary paleoclimate of northern margins of the saharan-arabian desert: reconstruction from speleothems of Negev Desert, Israel. Quat. Sci. Rev. 29, 2647–2662. https://doi.org/10.1016/j.quascirev.2010.06.014.
Verheyden, S., Nader, F.H., Cheng, H.J., Edwards, L.R., Swennen, R., 2008.

Paleoclimate reconstruction in the Levant region from the geochemistry of a Holocene stalagmite from the Jeita cave, Lebanon. Quat. Res. 70, 368–381. https://doi.org/10.1016/j.yqres.2008.05.004.
Waldmann, N., Stein, M., Ariztegui, D., Starinsky, A., 2009. Stratigraphy, depositional environments and level reconstruction of the last interglacial Lake Samra in the Dead Sea basin. Quat. Res. 72, 1–15. https://doi.org/10.1016/j.yqres.2009.03.005.
Yas'ur, G., 2013. The Chronology of the Middle and Upper Paleolithic in the Western Galilee Based on U-Th Ages of Speleothems from Manot Cave, Israel. Hebrew University of Jerusalem.